

Supplementary Material

**Structures of purine nucleosidase from *Trypanosoma brucei*  
bound to isozyme-specific trypanocidals and a novel  
metalorganic inhibitor**

Francesca Giannese<sup>a</sup>, Maya Berg<sup>b</sup>, Pieter Van der Veken<sup>b</sup>, Valeria Castagna<sup>a</sup>, Paola Tornaghi<sup>a</sup>, Koen Augustyns<sup>b</sup>, and Massimo Degano<sup>a,\*</sup>

<sup>a</sup>Biocrystallography Unit, Department of Immunology, Transplantation, and Infectious Diseases, Scientific Institute San Raffaele, via Olgettina 58, 20132 Milan – Italy.

<sup>b</sup>Laboratory of Medicinal Chemistry, University of Antwerp, Universiteitsplein 1, 2610 Antwerp, Belgium

Correspondence email: [degano.massimo@hsr.it](mailto:degano.massimo@hsr.it)

Supplementary Table 1. Differences in molar absorption between nucleosides and nucleobases used in the kinetic assays of the *T. brucei brucei* IAGNH.

Nucleoside	Wavelength (nm)	$\Delta\epsilon$ (mM <sup>-1</sup> ·cm <sup>-1</sup> )
Inosine	280	-0.82
Adenosine	280	-2.0
Guanosine	260	-4.0
Cytidine	295	-0.44
p-NPR <sup>a</sup>	400	12.0

<sup>a</sup>p-NPR, para-nitrophenyl riboside

Supplementary Table 2. Crystallization conditions for unliganded IAGNH and its complexes with competitive and noncompetitive inhibitors. See main text for abbreviations.

Protein-Ligands	Code	Buffer
IAGNH	-	0.2 M ammonium acetate pH 4.8, 18% PEG3350
IAGNH + Immucillin A	IAGNH-ImmA	0.1 M Tris pH 7.2, 22% PEGMME 2000, 10 mM NiSO <sub>4</sub>
IAGNH + UAMC-00363	IAGNH-363	0.1 mM Tris pH 8, 19% PEGMME 2000, 10 mM NiSO <sub>4</sub>
IAGNH + UAMC-00312	IAGNH-312	0.1 M Tris pH 7.3, 19% PEGMME 2000, 10 mM NiSO <sub>4</sub>
IAGNH + NiTris	IAGNH-NiTris	0.1 M Tris pH 8.6, 23% PEGMME 2000, 10 mM NiSO <sub>4</sub>
IAGNH + UAMC-00312 + Ni <sup>2+</sup>	IAGNH-312-M	0.1 M Tris pH 7.6, 23% PEGMME 2000, 10 mM NiSO <sub>4</sub>

Supplementary Table 3. Inhibition of IAGNH by iminoribitol-containing compounds.

The structures of the individual inhibitors are reported in Supplementary Figure 1.

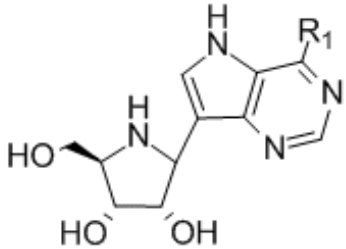
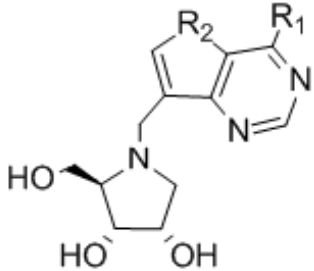
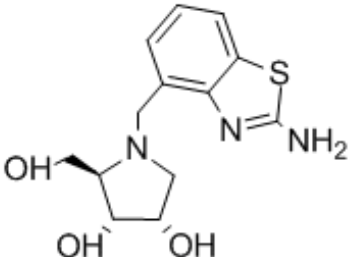
	K <sub>i</sub> (nM)		
	<i>Tbb</i> IAG-NH <sup>a</sup>	<i>Tbb</i> IG-NH <sup>b</sup>	<i>Tv</i> IAG-NH <sup>c</sup>
ImmA	0.9	4.4	6.2
ImmH	24	9	6.2
UAMC00363	18	32·10 <sup>3</sup>	4.1
UAMC00312	190	120·10 <sup>3</sup>	20
UAMC00115	446	11·10 <sup>3</sup>	11
UAMC00109	30	138·10 <sup>3</sup>	4.4
UAMC00311	560	31·10 <sup>3</sup>	40
UAMC00375	56	14·10 <sup>3</sup>	19

<sup>a</sup> Data taken from (Miles *et al.*, 1999)

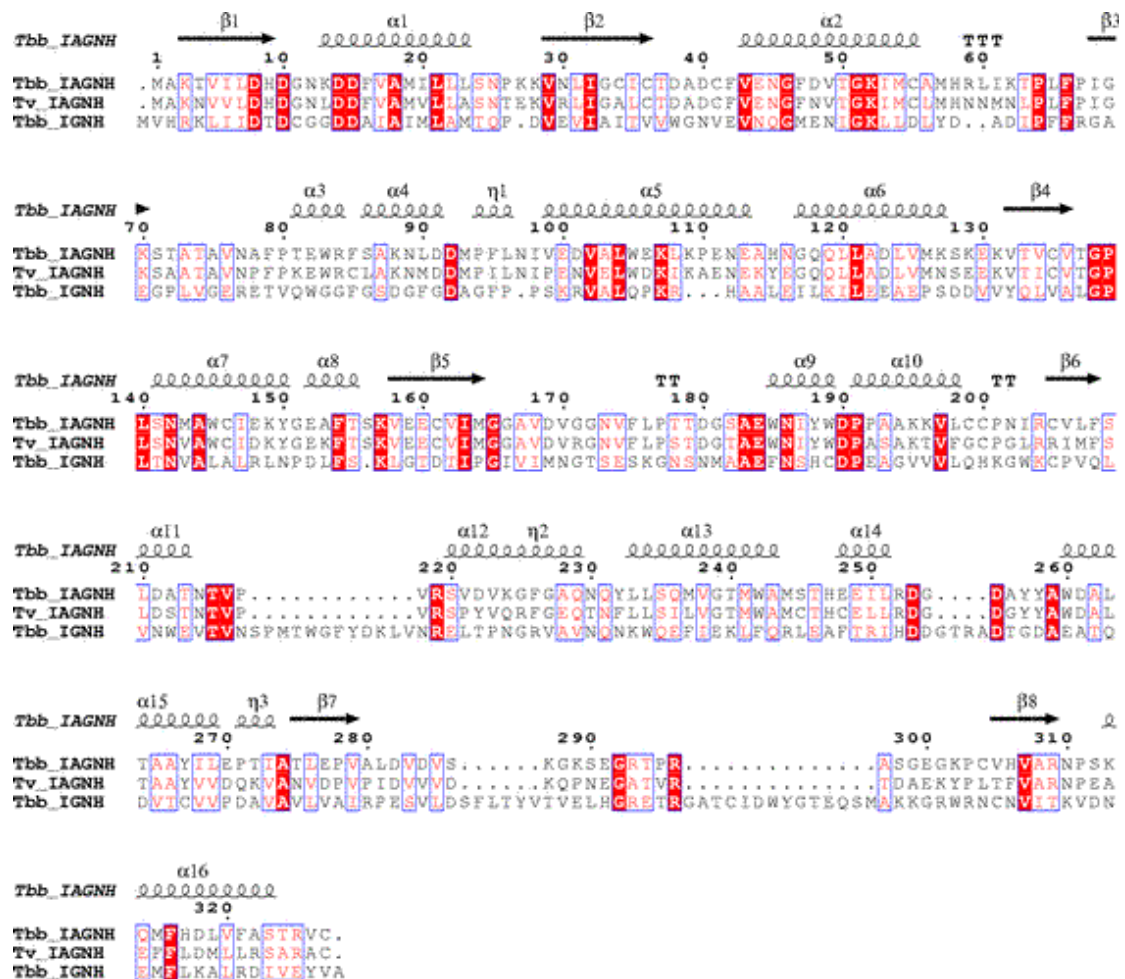
<sup>b</sup> Data taken from (Berg *et al.*, 2010)

<sup>c</sup> Data taken from (Versees *et al.*, 2006; Berg *et al.*, 2009; Goeminne *et al.*, 2008)

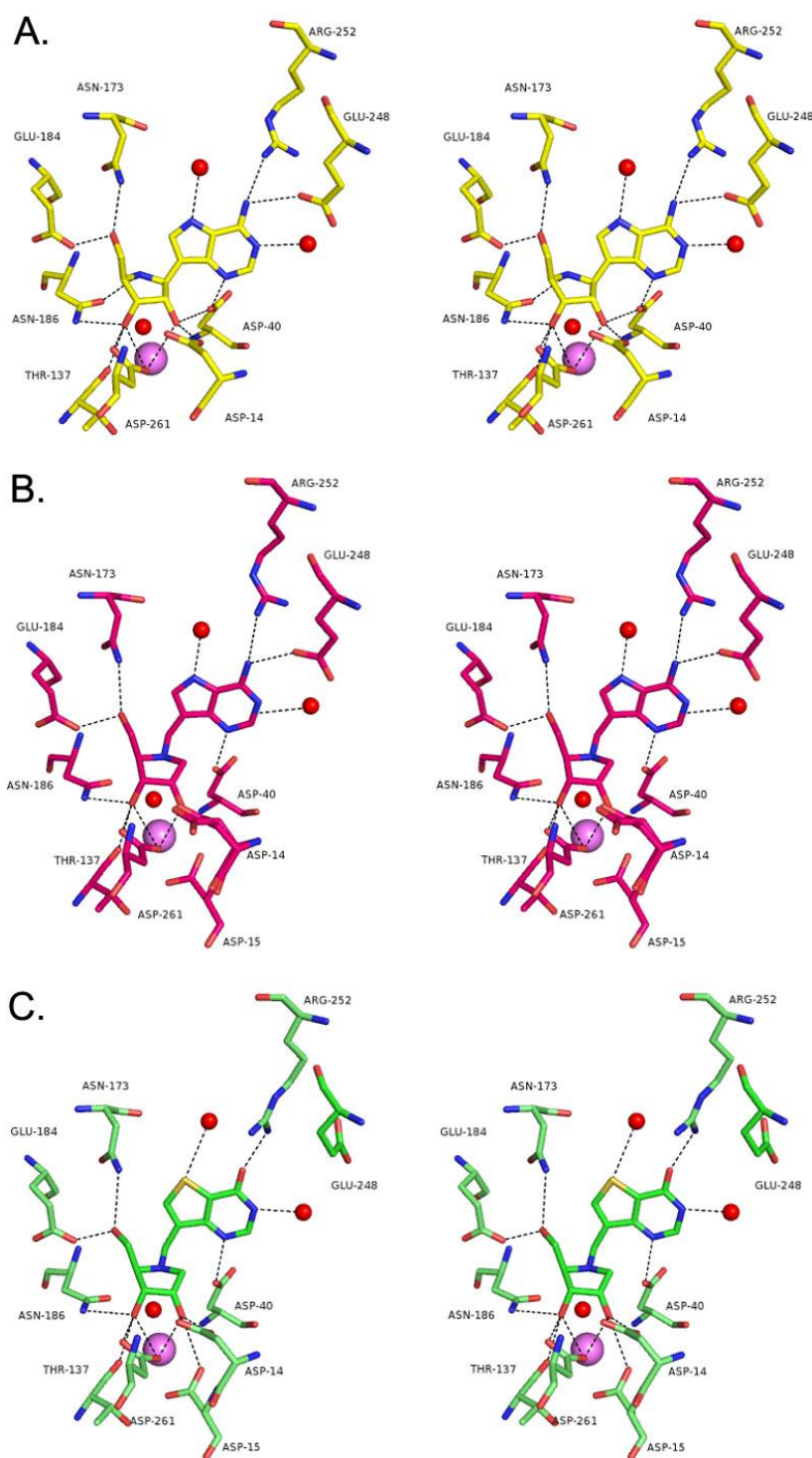
Supplementary figure 1. Structures of IAGNH inhibitors, and their inhibition constants against *Tbb* IAG-NH.

		R <sub>1</sub>	K <sub>i</sub> (nM)	
	ImmA	NH <sub>2</sub>	0.9	
	ImmH	OH	24	
		R <sub>1</sub>	R <sub>2</sub>	K <sub>i</sub> (nM)
	UAMC-00363	NH <sub>2</sub>	NH	18
	UAMC-00312	OH	S	190
	UAMC-00109	OH	NH	30
	UAMC-00375	NH <sub>2</sub>	S	56
				K <sub>i</sub> (nM)
	UAMC-003311			560

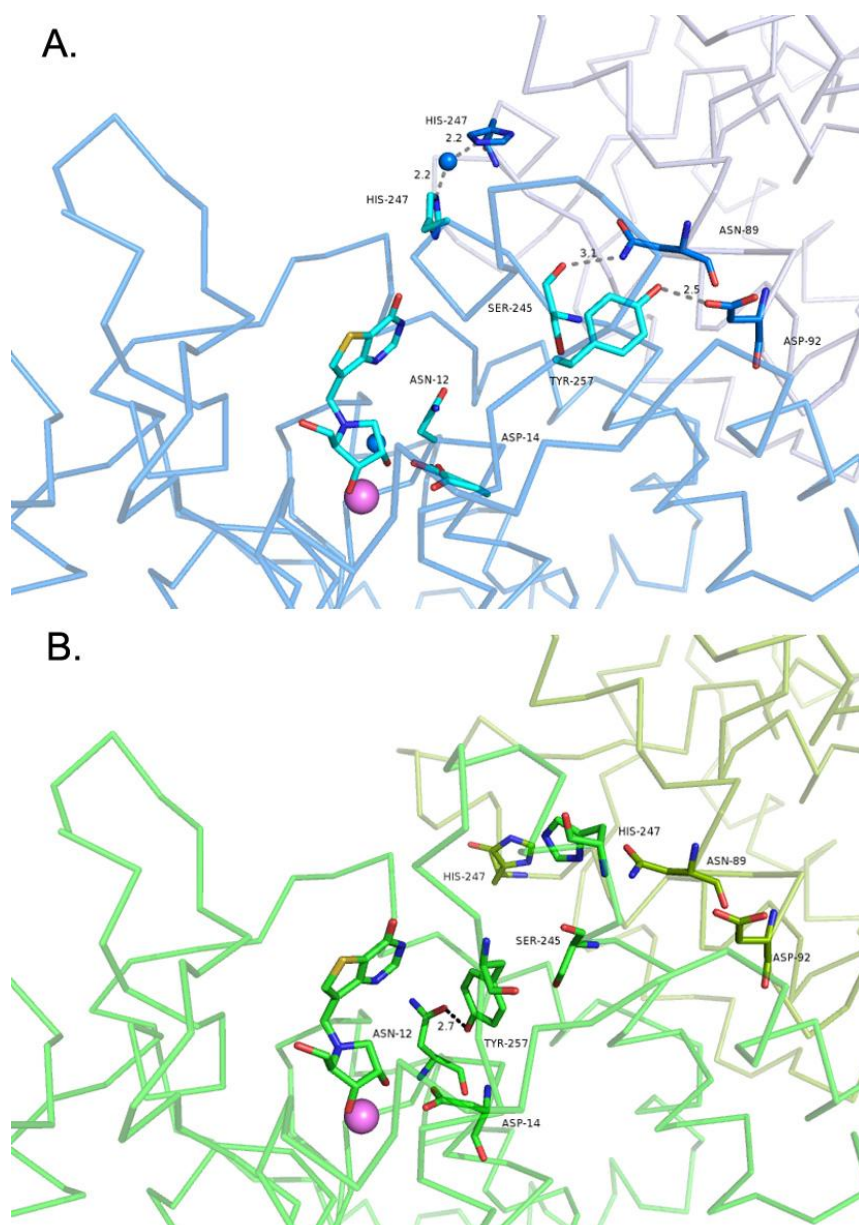
Supplementary Figure 2. Amino acid sequence alignment between *T. brucei* and *T. vivax* IAGNHs, and the *T. brucei* IAGNH. Secondary structure elements, as calculated using the program DSSP (Kabsch & Sander, 1983) on the IAGNH-363 complex, are indicated in the top row and numbered sequentially ( $\alpha$ = $\alpha$ -helix,  $\beta$ = $\beta$ -strand,  $\eta$ = $3_{10}$  helix, T=turn). Figure prepared using the program ESPRIPT (Gouet *et al.*, 1999).



Supplementary Figure 3. Different modes of inhibitor binding to IAGNH. Interactions between residues in the IAGNH active site cavity and (A) ImmA (B) 363 (C) 312. Hydrogen bonds are depicted as dashed lines. In each panel, nitrogen atoms are colored blue, oxygen atoms in red.

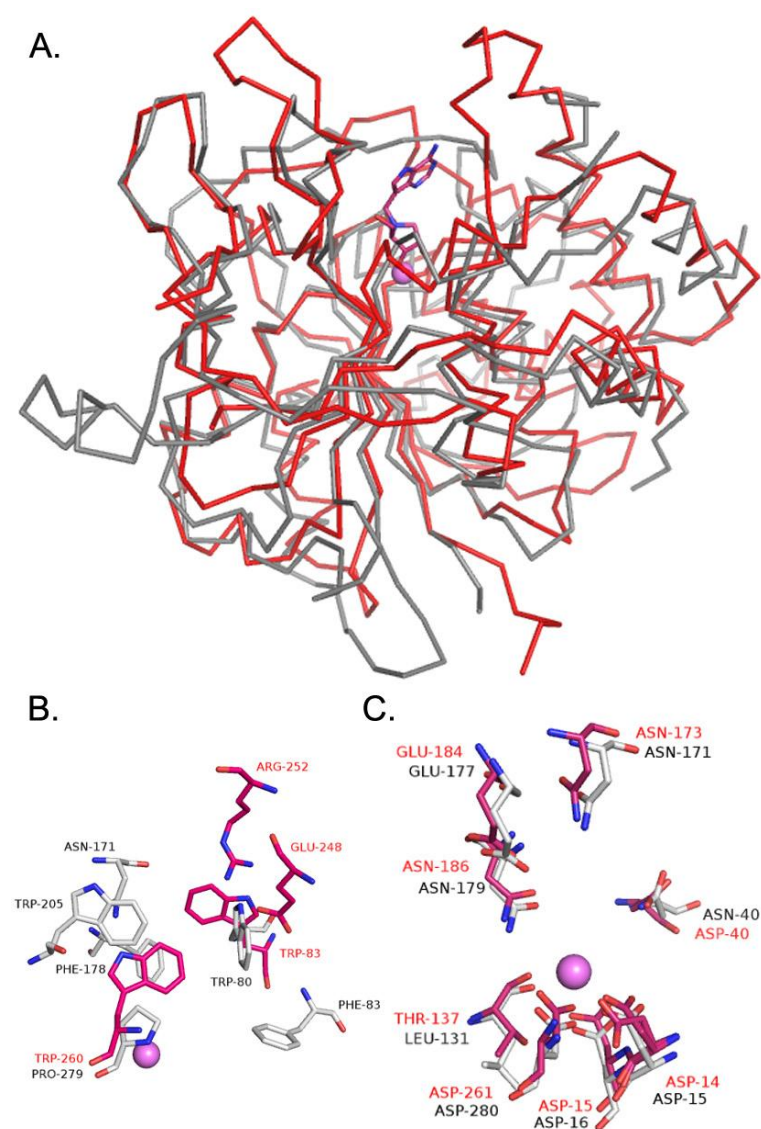


Supplementary Figure 4. Different intermolecular contacts at the monomer-monomer interface of the IAGNH-312-M and IAGNH-312 complexes. (A) Binding of the noncompetitive inhibitor  $\text{Ni}^{2+}$  (blue sphere) to the IAGNH modifies the loop 2 conformation, and leads to the formation of hydrogen bonds between residues Asp92 with Tyr257, and Asn89 with Ser245. (B) For comparison, the structure of IAGNH bound to the same inhibitor, but with no ion bound at the noncompetitive site. Tyr257 is hydrogen bonded to Asn12 of the same monomer, and stabilizes the catalytic conformation.



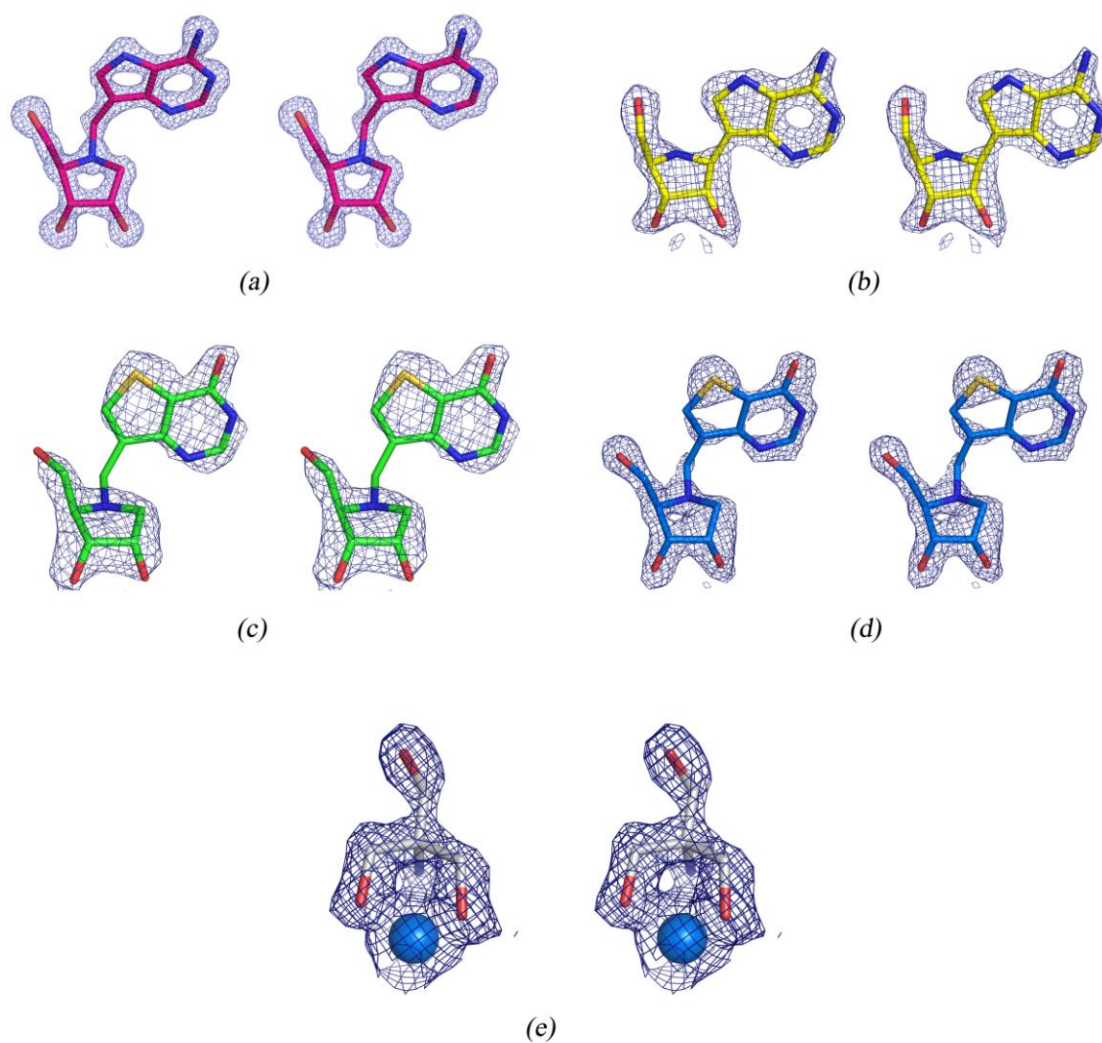


Supplementary figure 5. Comparison between IAGNH and IGNH from *T. brucei*. (A) Superposition of the Ca traces of the IAGNH (complex with compound 363, red) and IGNH (bound to BisTris, grey) monomer (Minici *et al.*, 2012). (B) Residues interacting with the active site  $\text{Ca}^{2+}$  ion and the ribose moiety of substrates (shown as stick models, same color scheme) are conserved in the two NH enzymes. (C) The residues interacting with the nitrogenous base of nucleoside substrates differ between the two enzymes, both in nature and, when conserved, in orientation.



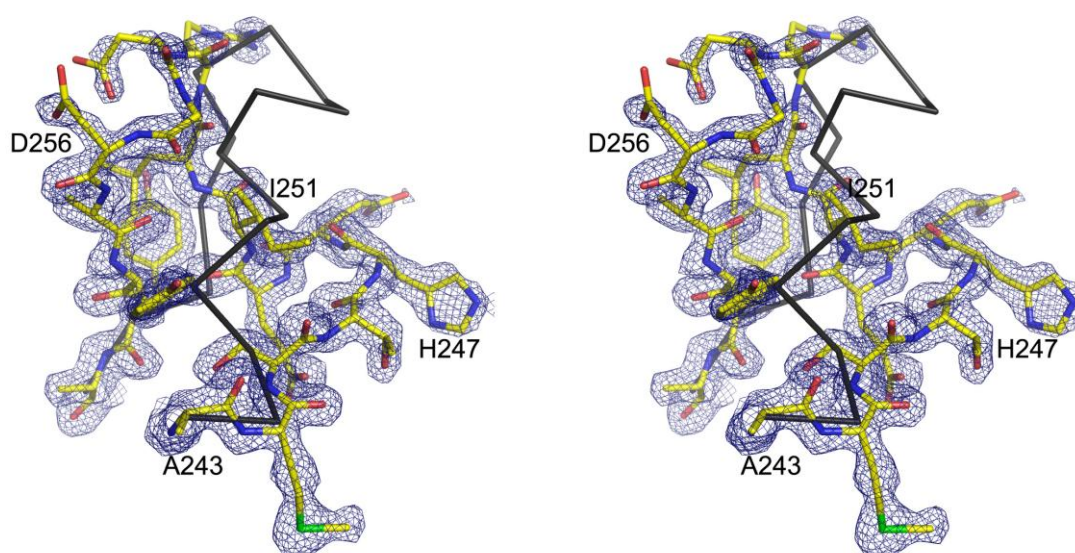
Supplementary Figure 6.

Electron densities for ligands of the the IAGNH complexes. Stereoscopic projections of the (a) UAMC-363, (b) ImmA, (c) UAMC-312, (d) UAMC-312 in the 312M complex, and (e) Ni-Tris inhibitor structures in the refined models with the electron density map shown as a blue mesh and contoured at  $1.5\sigma$ , except for UAMC-363 where the contour is set at  $2\sigma$ . The maps were calculated using sigmaa-weighted 2mFo-DFc coefficients and model phases before the inclusion of the ligands in the refinement.



Supplementary Figure 7.

Omit electron density for the loop in the 312M structure. The amino acid residues of the loop in the IAGNH-312-Ni complex are shown as sticks. The electron density is contoured at  $1.0\sigma$ , and was calculated with 2mFo-DFc coefficients and model phases after omitting the region shown and applying a random perturbation to the coordinates to a final 0.25 Å rmsd. In black, the C $\alpha$  trace of the IAGNH in complex with compound UAMC-363 is shown to underscore the different conformation of the region.



## References.

- Berg, M., Bal, G., Goeminne, A., Van der Veken, P., Versees, W., Steyaert, J., Haemers, A. & Augustyns, K. (2009). *ChemMedChem* **4**, 249-260.
- Berg, M., Kohl, L., Van der Veken, P., Joossens, J., Al-Salabi, M. I., Castagna, V., Giannese, F., Cos, P., Versees, W., Steyaert, J., Grellier, P., Haemers, A., Degano, M., Maes, L., de Koning, H. P. & Augustyns, K. (2010). *Antimicrob Agents Chemother* **54**, 1900-1908.
- Goeminne, A., Berg, M., McNaughton, M., Bal, G., Surpateanu, G., Van der Veken, P., De Prol, S., Versees, W., Steyaert, J., Haemers, A. & Augustyns, K. (2008). *Bioorg Med Chem* **16**, 6752-6763.
- Gouet, P., Courcelle, E., Stuart, D. I. & Metoz, F. (1999). *Bioinformatics* **15**, 305-308.
- Kabsch, W. & Sander, C. (1983). *Biopolymers* **22**, 2577-2637.
- Miles, R. W., Tyler, P. C., Evans, G. B., Furneaux, R. H., Parkin, D. W. & Schramm, V. L. (1999). *Biochemistry* **38**, 13147-13154.
- Minici, C., Cacciapuoti, G., De Leo, E., Porcelli, M. & Degano, M. (2012). *Biochemistry* **51**, 4590-4599.
- Versees, W., Barlow, J. & Steyaert, J. (2006). *J Mol Biol* **359**, 331-346.